Electronic Supplementary Material (ESI) for Journal of Materials Chemistry C.

Supporting information for

Black-Phosphorus-Analogue Tin Monosulfide: An Emerging Optoelectronic Two-Dimensional Material for High-Performance Photodetection with Improved Stability under Ambient/Harsh Conditions

Weichun Huang,‡[a] Zhongjian Xie,‡[a] Taojian Fan,[a] Jiagen Li,[b] Yunzheng Wang,[a] Leiming Wu,[c] Dingtao Ma,[c] Zhongjun Li,[c] Yanqi Ge,[a] Ziyin N. Huang,[d] Xiaoyu Dai,[a] Yuanjiang Xiang,[a] Jianqing Li,[c] Xi Zhu,*[b] and Han Zhang*[a]

[a.] Collaborative Innovation Centre for Optoelectronic Science & Technology, and Key Laboratory of Optoelectronic Devices and Systems of Ministry of Education and Guangdong Province, College of Optoelectronic Engineering, Shenzhen University, Shenzhen 518060, China.

[b.] School of Science and Engineering, The Chinese University of Hong Kong, Shenzhen, Shenzhen 518172, China.

[c.] Faculty of Information Technology, Macau University of Science and Technology, Macao 519020, P. R. China.

[d.] Department of Materials Science and Engineering, Northwestern University, Evanston, IL 60208, USA

Table S1 Size-dependent Raman peak positions of bulk SnS and 2D SnS Ns.

	B_{3g}/cm^{-1}	A_g/cm^{-1}	A_{3u}/cm^{-1}
Bulk SnS	162.3	191.4	220.1
$SnS_{2\text{-}4K}$ Ns	159.9	188.6	219.1
$SnS_{4\text{-}6K}$ Ns	158.3	188.3	217.5
$SnS_{6\text{-}8K}$ Ns	157.5	187.3	217.4

Table S2 The light powder density (P_λ) of incident light with various irradiation wavelengths. The gradually increased P_λ were labelled with I, II, III, IV, and VI levels, respectively.

P_λ (mW/cm^2)	I level	II level	III level	IV level	VI level
Simulated light (SL)	26.2	53.0	83.1	118	122
365 nm	0.764	1.66	2.55	3.57	3.69
400 nm	0.637	2.04	3.57	5.22	5.35
475 nm	1.91	4.33	7.01	10.1	10.6
550 nm	2.04	3.95	5.98	8.28	8.40
650 nm	2.04	4.08	6.02	8.54	8.92
700 nm	1.15	2.42	4.08	6.11	6.14

Table S3 R_s in different concentration of Na_2SO_4 at bias voltages of 0 V, 0.3 V and 0.6 V.

	R_s/Ω
0.1 M Na_2SO_4 (0 V)	15.5 ± 0.1
0.5 M Na_2SO_4 (0 V)	6.54 ± 0.12
0.5 M Na_2SO_4 (0.3 V)	6.55 ± 0.10
0.5 M Na_2SO_4 (0.6 V)	6.52 ± 0.09
1.0 M Na_2SO_4 (0 V)	4.87 ± 0.07

Table S4 R_s in 0.5 M electrolytes at a bias voltage of 0 V.

	0.5 M H_2SO_4	0.5 M Na_2SO_4	0.5 M KOH
Rs/Ω	7.12 ± 0.07	6.53 ± 0.04	5.29 ± 0.09

Table S5 *D** values of the 2D $SnS_{4\text{-}6K}$ Ns-based photodetector in 0.5 M different electrolytes at 0.6 V at IV level under SL and irradiation with different wavelengths. *D** is given in Jones (cm $Hz^{1/2}$ W^{-1}).

	0.5 M H_2SO_4	0.5 M Na_2SO_4	0.5 M KOH
SL	1.43×10^7	9.43×10^7	1.85×10^6
365 nm	9.45×10^7	1.92×10^8	2.74×10^6
400 nm	5.17×10^7	7.55×10^7	3.84×10^6
475 nm	2.08×10^7	2.43×10^7	1.82×10^6
550 nm	1.38×10^7	1.65×10^7	-[a]
650 nm	8.31×10^6	1.08×10^7	-[a]

[a] Data not available as the corresponding values of photoresponsivity are negligible.

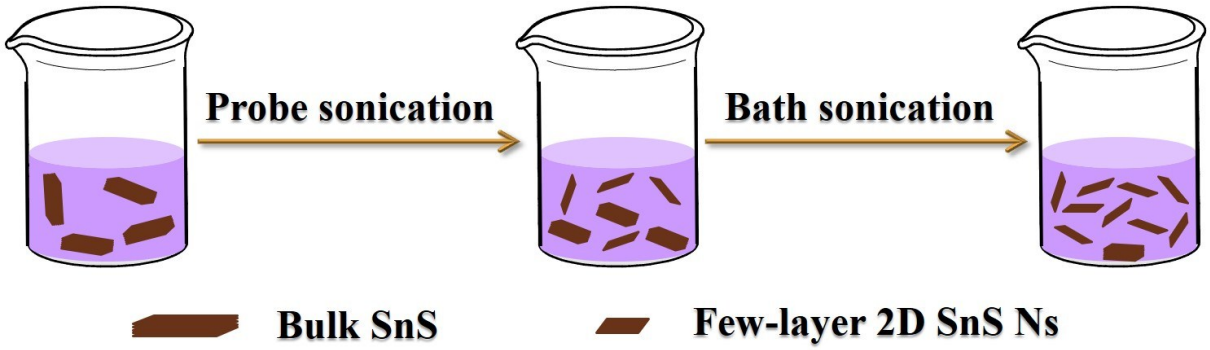

Scheme S1. A LPE strategy to fabricate the 2D SnS Ns.

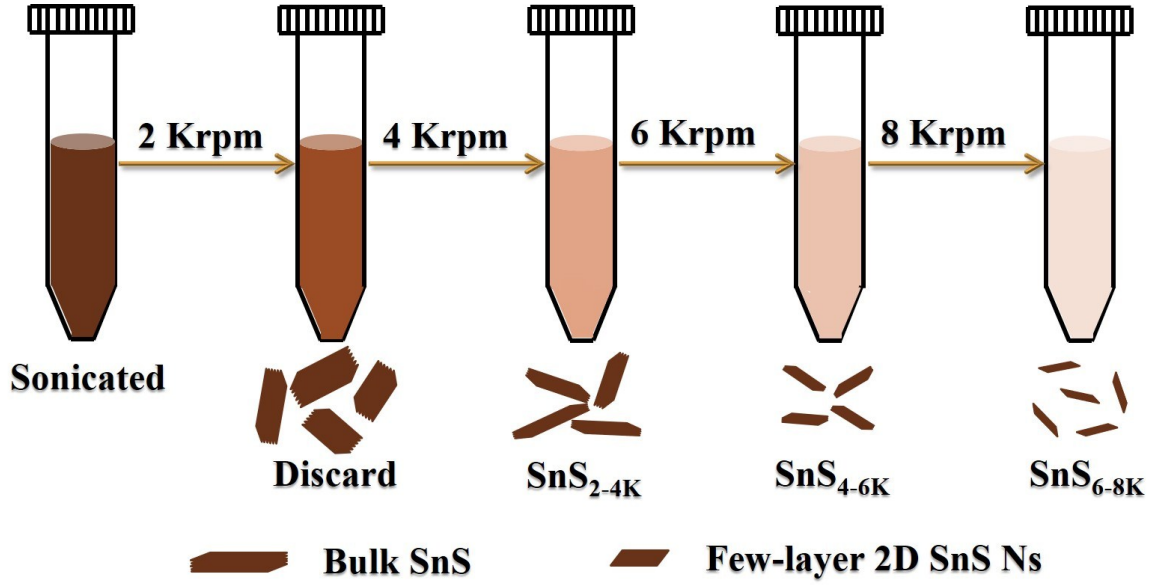

Scheme S2. Schematic describing the basic centrifugation cascade employed in this study.

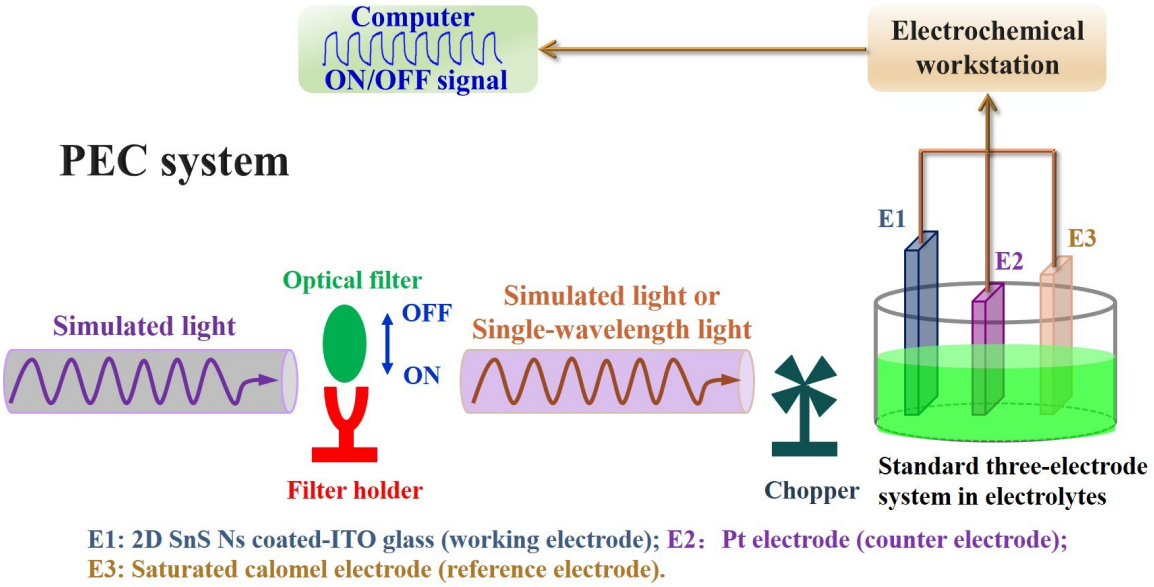

Scheme S3. A typical PEC system built for evaluating the photoresponse behavior of the 2D SnS Ns-based photodetector in electrolytes.

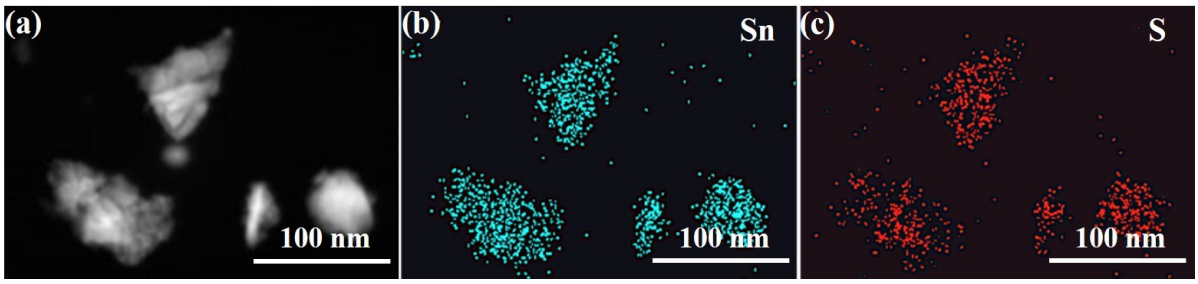

Fig. S1. (a) TEM images of some single SnS Ns. (b and c) Energy dispersive X-ray (EDX) spectrum imaging of the same SnS Ns as in (a), showing the even distribution of tin and sulfur throughout the SnS Ns.

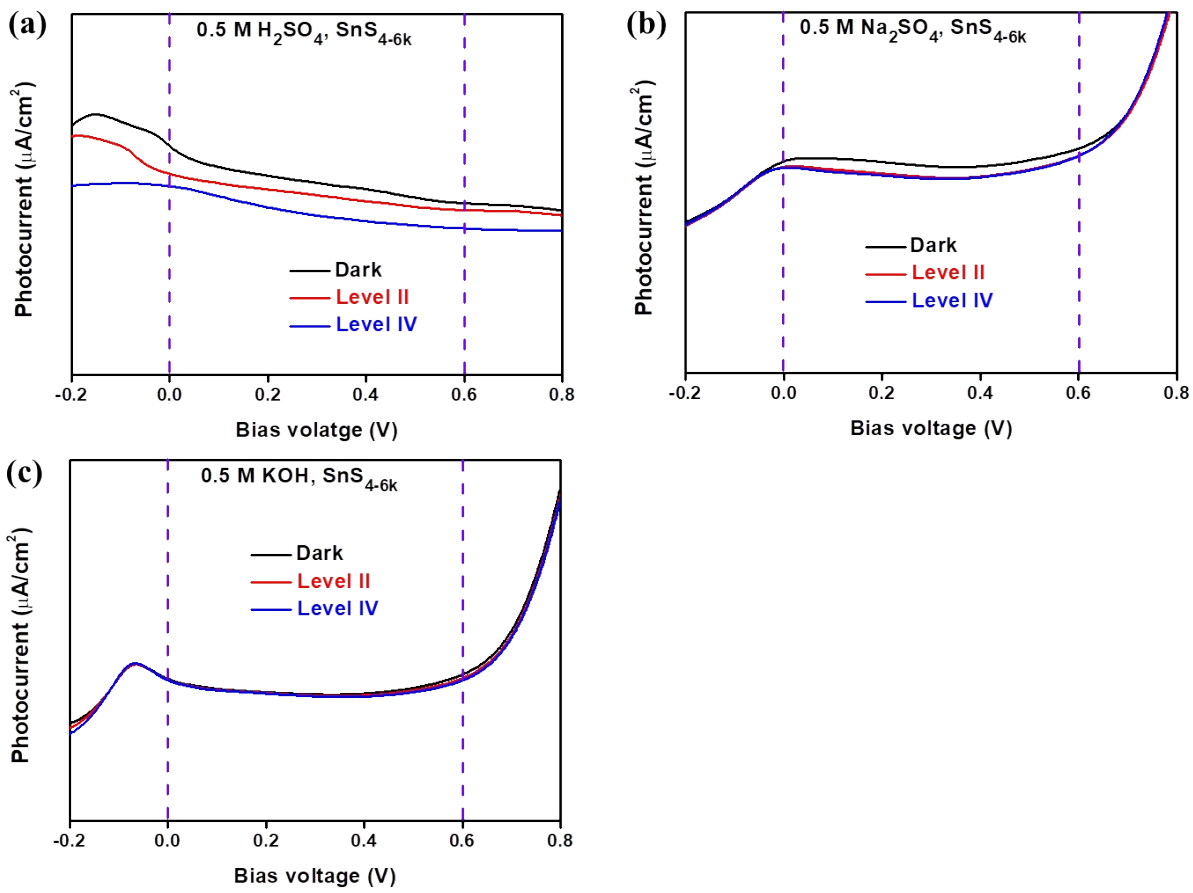

Figure S2. Linear sweep voltammetry curves of 2D $SnS_{4\text{-}6k}$ Ns-based photodetectors in 0.5 M various electrolytes under simulated light (a mixed light from 350 to 800 nm) with different power density, dark (0 mW/cm^2), level II (53.0 mW/cm^2) and level IV (118 mW/cm^2). (a) 0.5 M H_2SO_4, (b) 0.5 M Na_2SO_4 and (c) 0.5 M KOH.

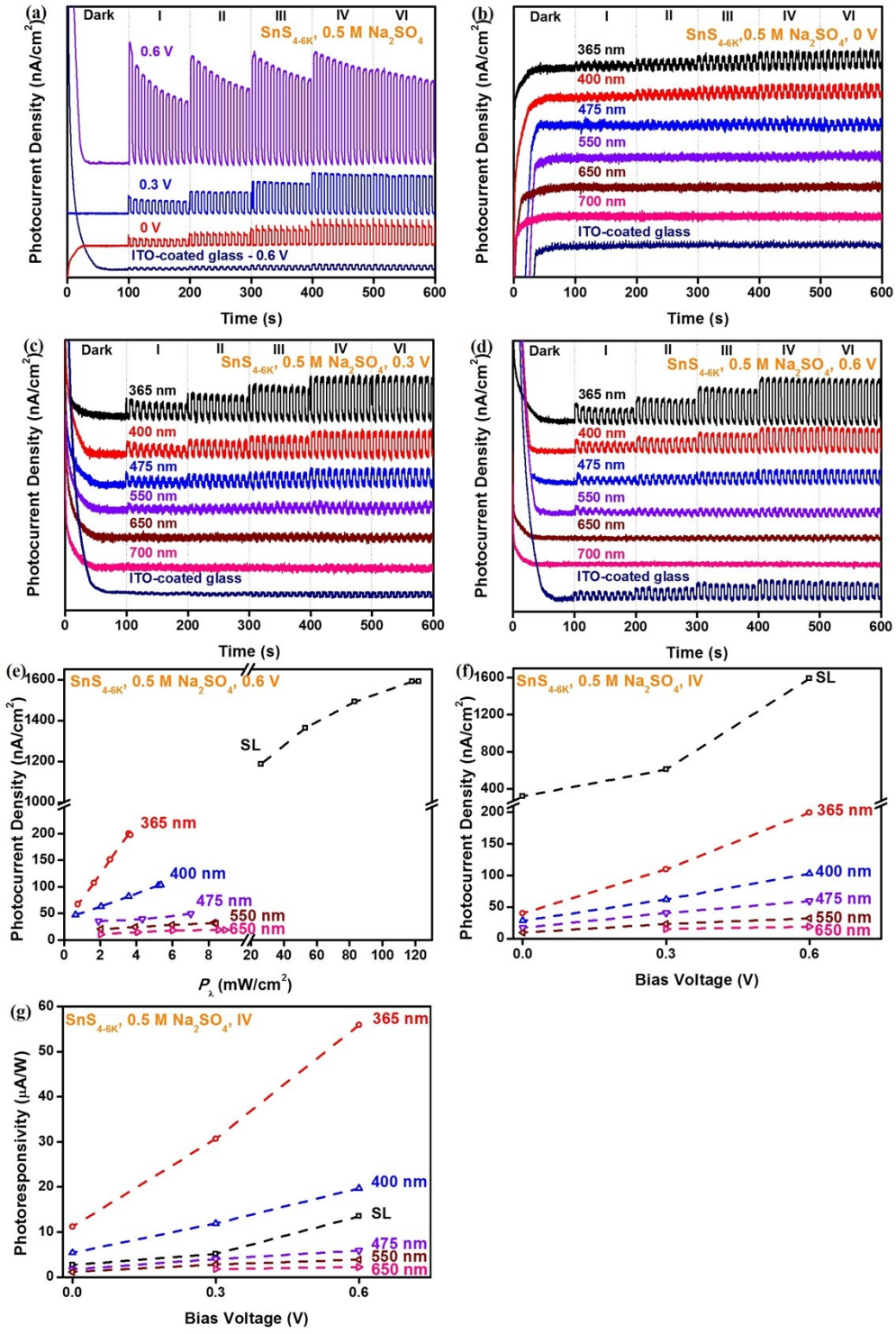

Fig. S3. Typical photoresponse behaviour of the 2D $SnS_{4\text{-}6k}$ Ns-based photodetector in 0.5 M Na_2SO_4 under illumination by SL and irradiation with various wavelengths. (a) ON/OFF switching behaviour triggered by irradiation with simulated light with increasing light power density from dark to VI level at voltages of 0, 0.3, and 0.6 V. (b-d) ON/OFF switching behaviour at voltages of (b) 0, (c) 0.3, and (d) 0.6 V under illumination with wavelengths of 365, 400, 475, 550, 650, and 700 nm. (e) Photocurrent density (P_{ph}) as a function of the light power density for SL and irradiation with various wavelengths. (f) P_{ph} as a function of the bias voltage for SL and irradiation with various wavelengths. (g) Photoresponsivity (R_{ph}) as a function of the bias voltage for SL and irradiation with various wavelengths.

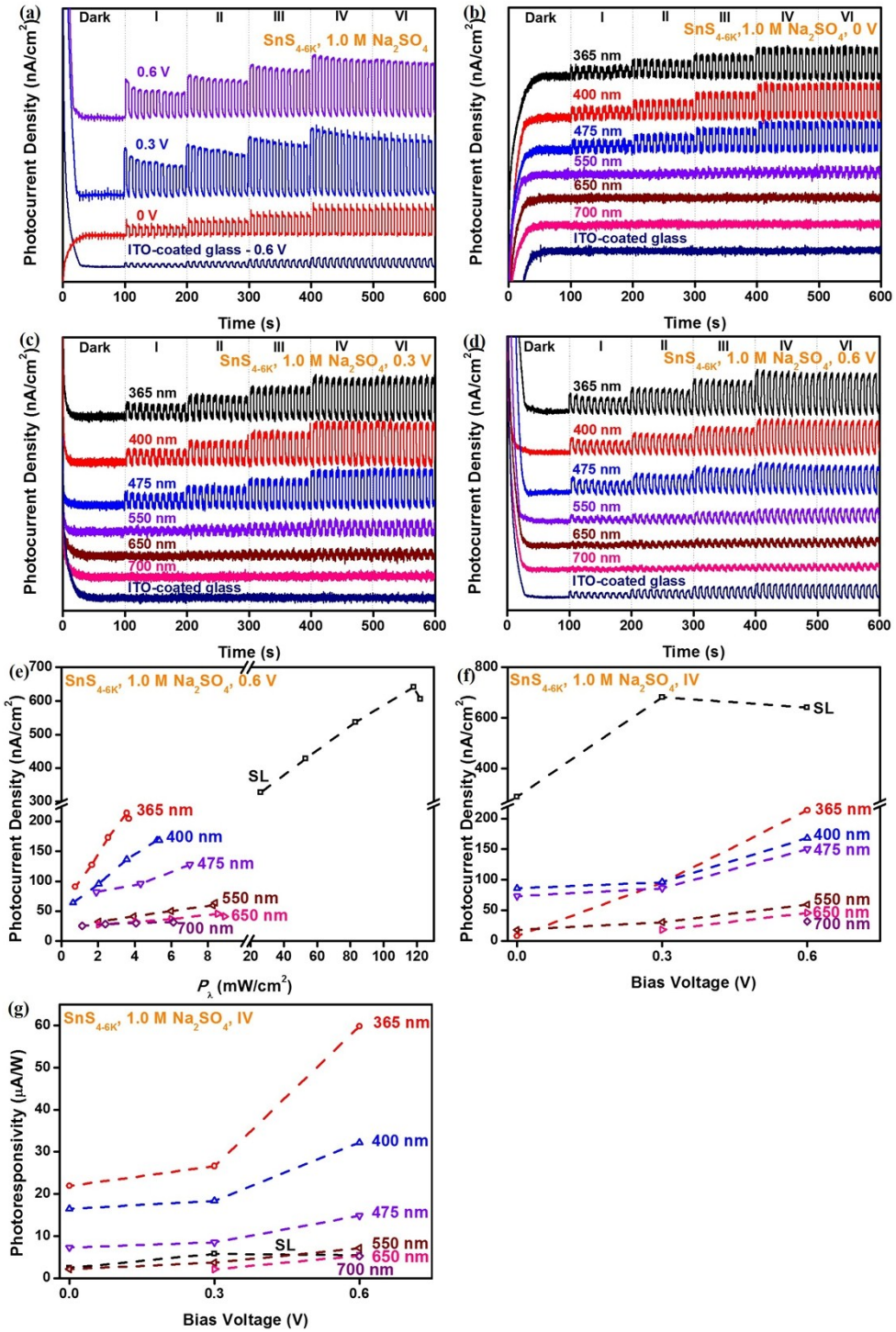

Fig. S4. Typical photoresponse behaviour of the 2D $SnS_{4\text{-}6k}$ Ns-based photodetector in 1.0 M Na_2SO_4 under illumination by SL and irradiation with various wavelengths. (a) ON/OFF switching behaviour triggered by irradiation with simulated light with increasing light power density from dark to VI level at voltages of 0, 0.3, and 0.6 V. (b-d) ON/OFF switching behaviour at voltages of (b) 0, (c) 0.3, and (d) 0.6 V under illumination with wavelengths of 365, 400, 475, 550, 650, and 700 nm. (e) Photocurrent density (P_{ph}) as a function of the light power density for SL and irradiation with various wavelengths. (f) P_{ph} as a function of the bias voltage for SL and irradiation with various wavelengths. (g) Photoresponsivity (R_{ph}) as a function of the bias voltage for SL and irradiation with various wavelengths.

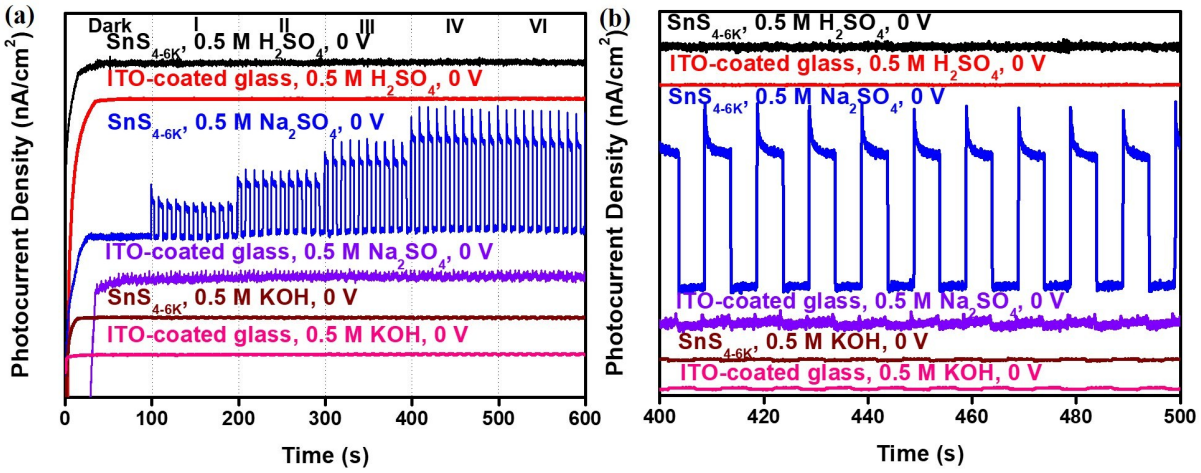

Fig. S5. (a) Self-powered behaviors of the 2D $SnS_{4\text{-}6k}$ Ns-based photodetector in 0.5 M different electrolytes (H_2SO_4, Na_2SO_4 and KOH) under illumination by SL with increasing light power density from dark to VI level, (b) the selected region in (a) under a light power density at IV level.

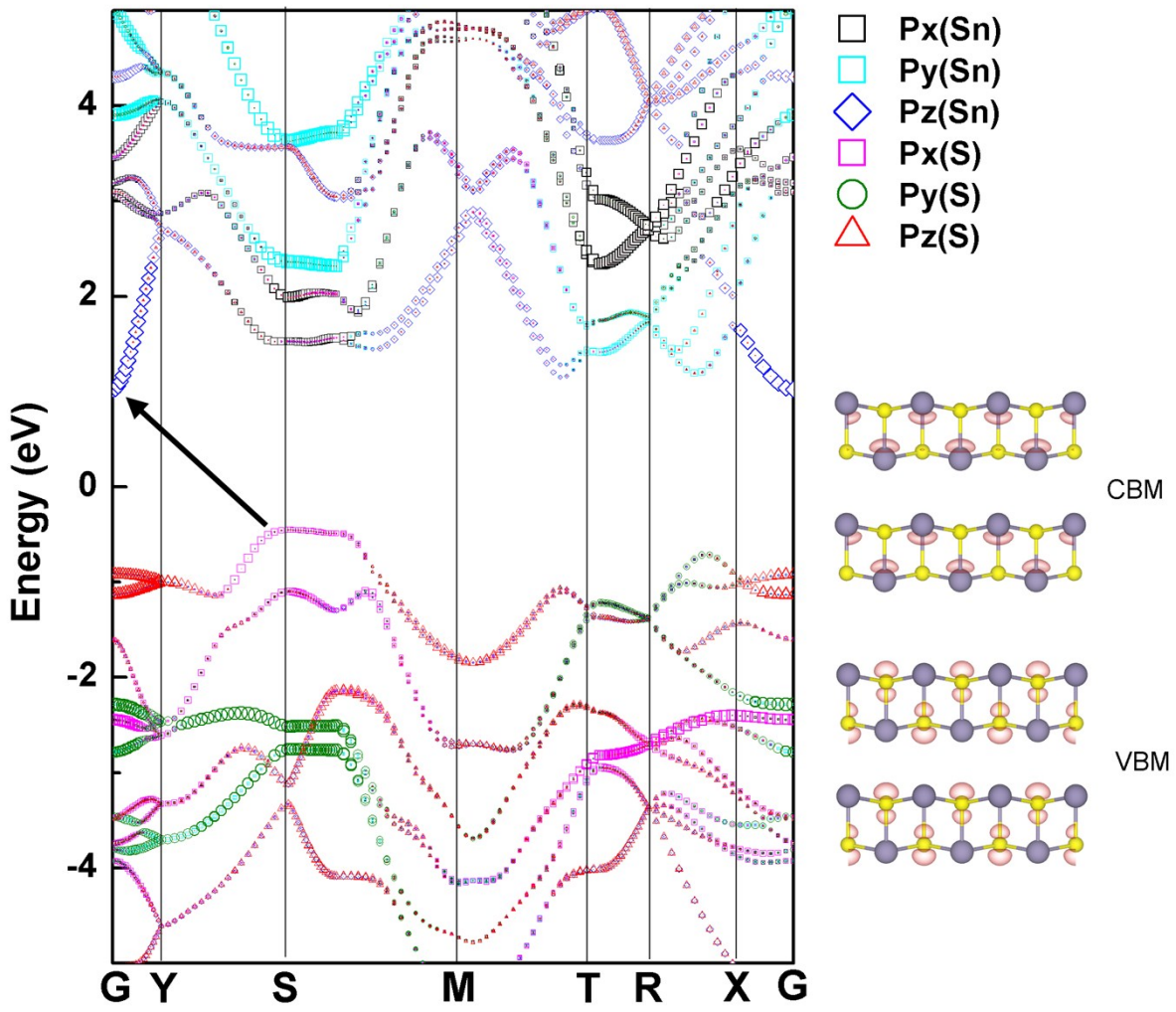

Fig. S6. The Density of states projected band structure and the valence band minimal (VBM) and conduction band maximal (CBM) for the 2L SnS layer strcture. The Sn and S atoms are colored in purple and yellow respectively. The black arrow indicates a bandgap energy of 1.56 eV.

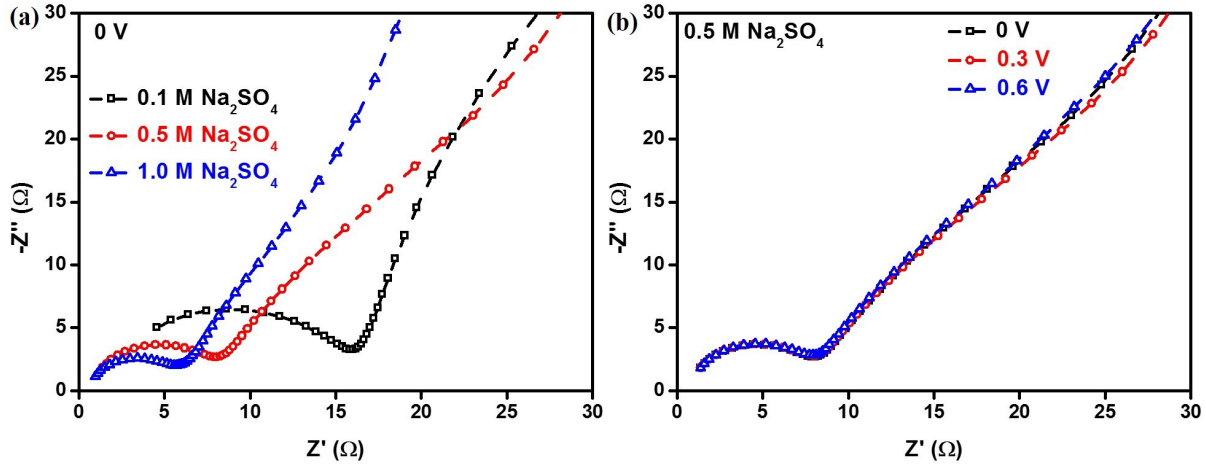

Fig. S7. Electrochemical impedance spectrum (EIS) investigations of the 2D $SnS_{4\text{-}6k}$ Ns-based photodetector (a) in various Na_2SO_4 concentrations and (b) under different applied bias potentials at IV level in 0.5 M Na_2SO_4.

The resistance R_s was read as the intersection of the linear fit with axis of real impedance part in the Nyquist plot (also consistent with the result obtained from the high-frequency plateau in the real impedance plot). Two to three measurements were performed for each sample.

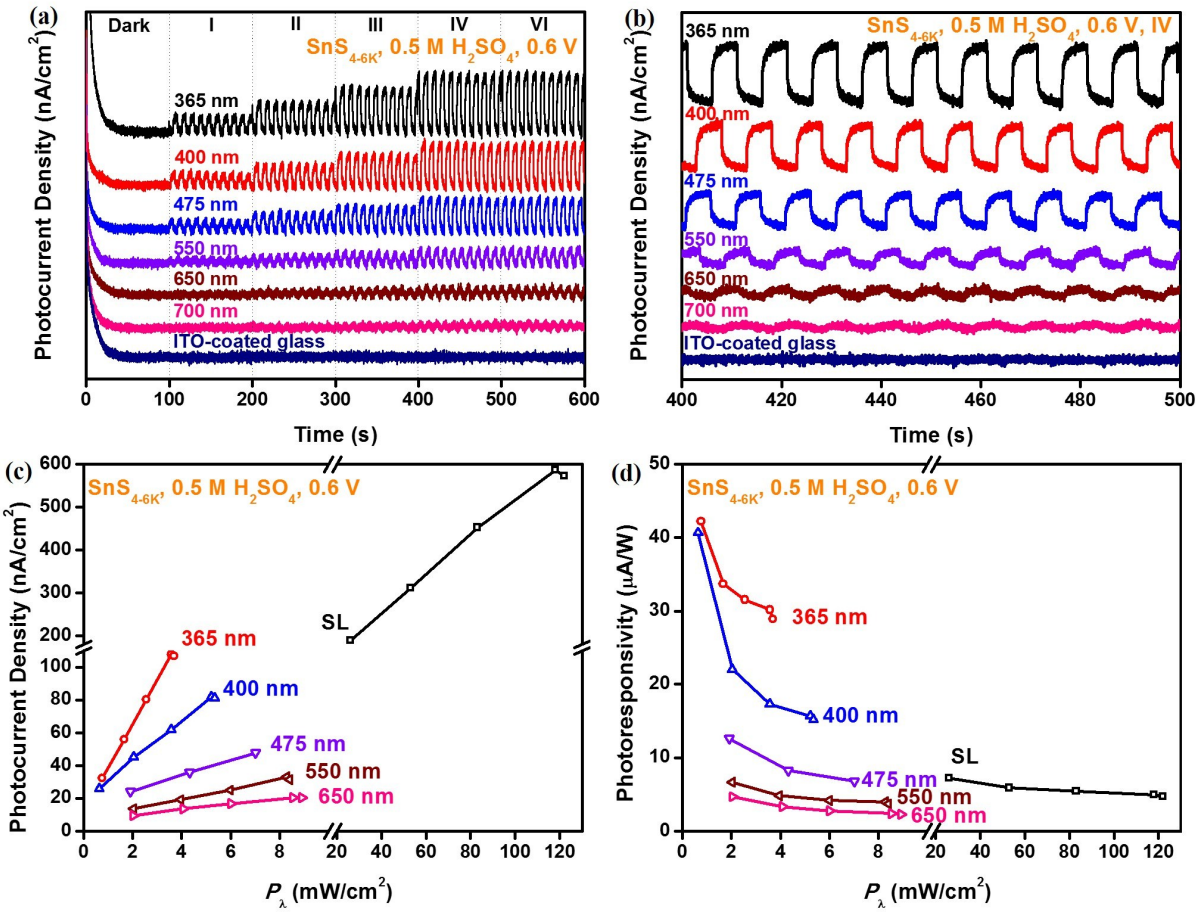

Fig. S8. (a) Typical photoresponse behaviour of the 2D $SnS_{4\text{-}6k}$ Ns-based photodetector in 0.5 M H_2SO_4 under illumination by irradiation with various wavelengths at 0.6 V, (b) the selected region in (a) by irradiation with various wavelengths at IV level. (c) Photocurrent density (P_{ph}) as a function of the power density for SL and irradiation with various wavelengths. (d) Photoresponsivity (R_{ph}) as a function of the power density for SL and irradiation with various wavelengths.

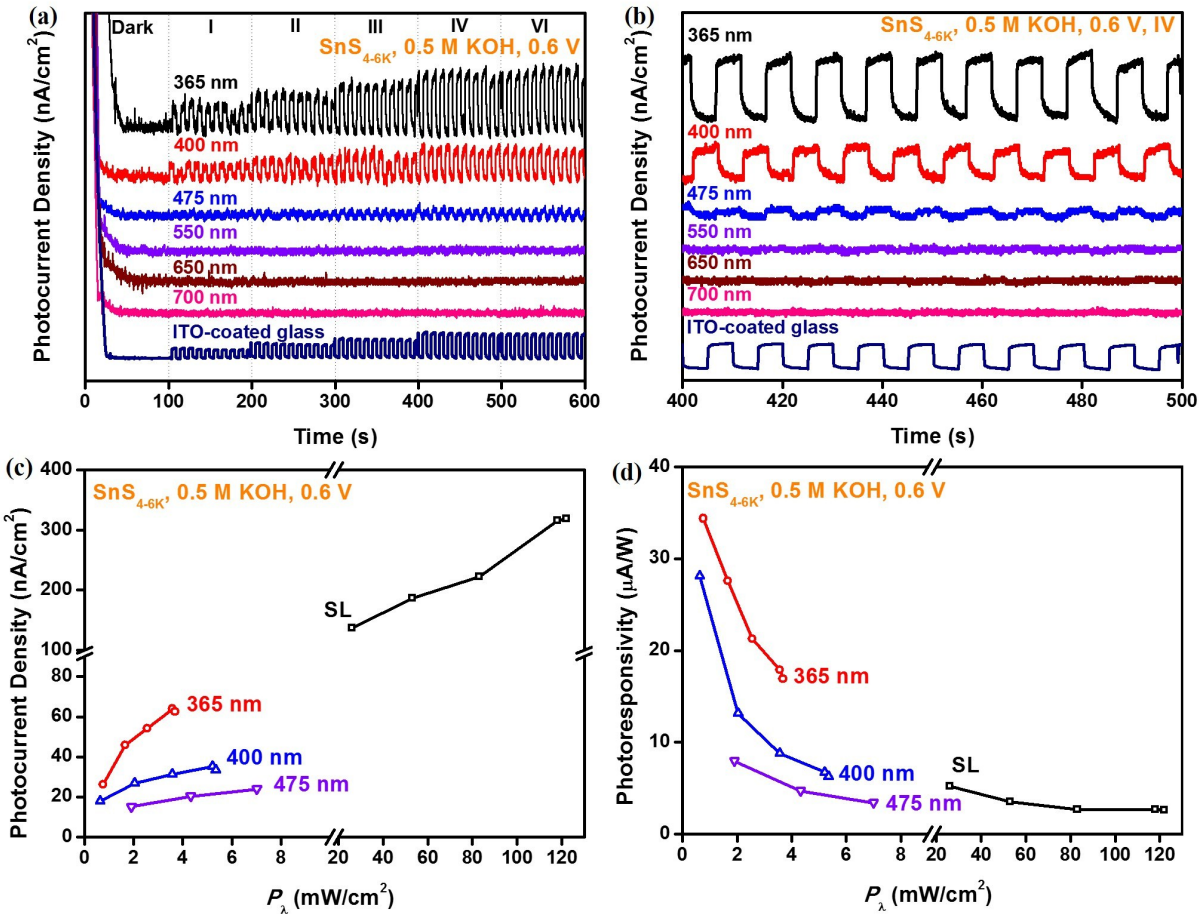

Fig. S9. (a) Typical photoresponse behaviour of the 2D $SnS_{4\text{-}6k}$ Ns-based photodetector in 0.5 M KOH under illumination by irradiation with various wavelengths at 0.6 V, (b) the selected region in (a) by irradiation with various wavelengths at IV level. (c) Photocurrent density (P_{ph}) as a function of the power density for SL and irradiation with various wavelengths. (d) Photoresponsivity (R_{ph}) as a function of the power density for SL and irradiation with various wavelengths.

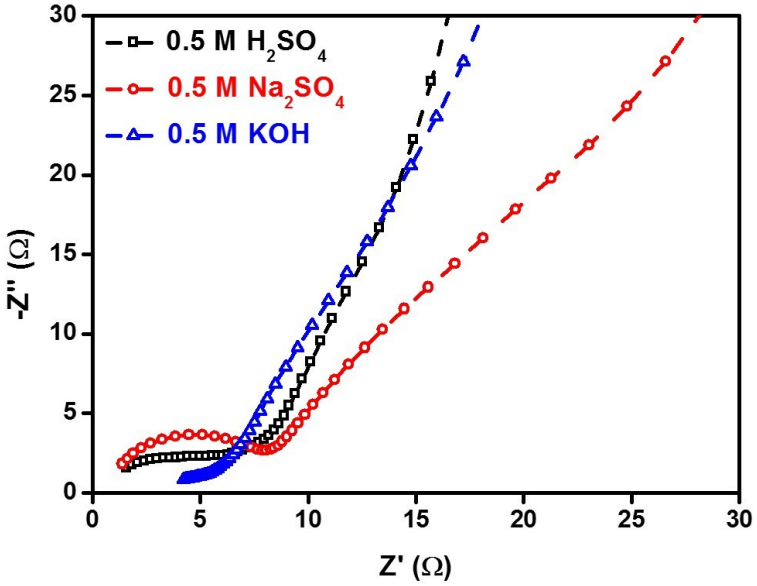

Fig. S10. Electrochemical impedance spectrum (EIS) investigations of the 2D $SnS_{4\text{-}6k}$ Ns-based photodetector in 0.5 M different electrolytes at 0 V.

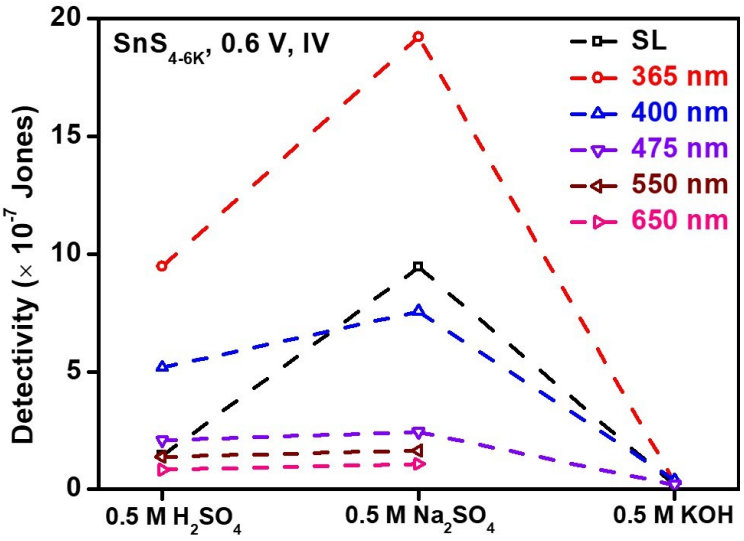

Fig. S11. Detectivity (*D**) of the 2D $SnS_{4\text{-}6k}$ Ns-based photodetector in 0.5 M different electrolytes at 0.6 V at IV level under SL and irradiation with different wavelengths.

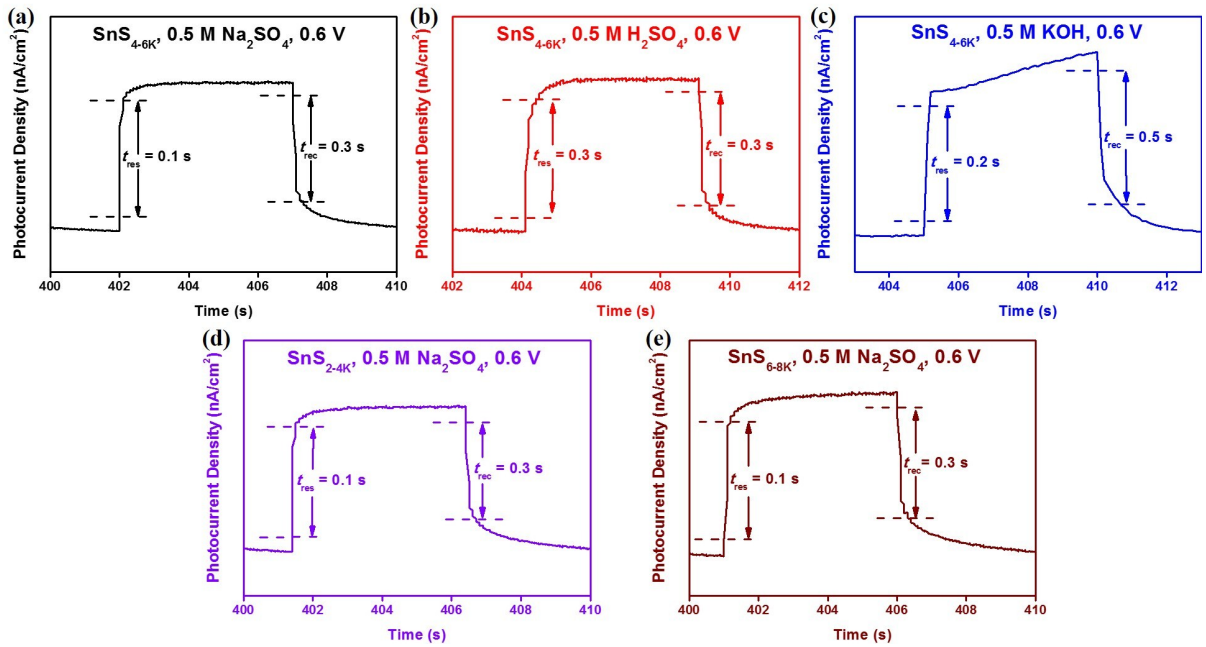

Fig. S12. The profiles of response time (t_{res}) and recovery time (t_{rec}) of the size-selected 2D SnS Ns-based photodetector in different electrolytes at the same IV level at 0.6 V under SL. (a)$SnS_{4\text{-}6k}$, 0.5 M Na_2SO_4; (b) $SnS_{4\text{-}6k}$, 0.5 M H_2SO_4; (c) $SnS_{4\text{-}6k}$, 0.5 M KOH; (d) $SnS_{2\text{-}4k}$, 0.5 M Na_2SO_4; (e) $SnS_{6\text{-}8k}$, 0.5 M Na_2SO_4.

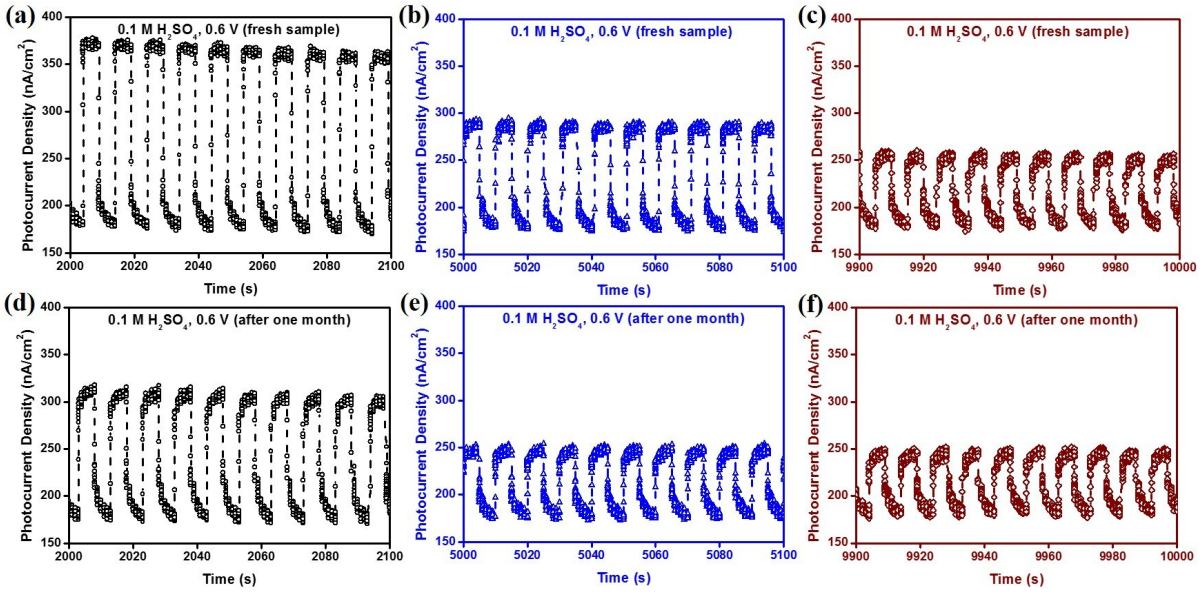

Fig. S13. Long-term stability of the photoresponse performance of the 2D $SnS_{2\text{-}4k}$ Ns-based photodetector under SL in 0.1 M H_2SO_4 (a-c) before and (d-f) after 1 month at 0.6 V at IV level.

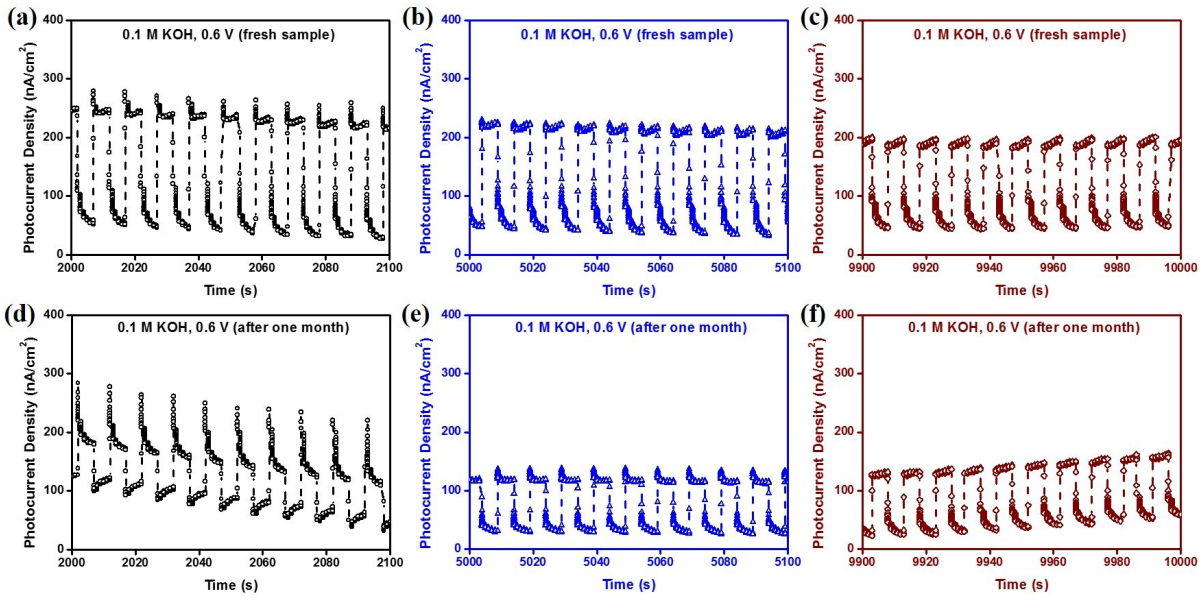

Fig. S14. Long-term stability of the photoresponse performance of the 2D $SnS_{2\text{-}4k}$ Ns-based photodetector under SL in 0.1 M KOH (a-c) before and (d-f) after 1 month at 0.6 V at IV level.

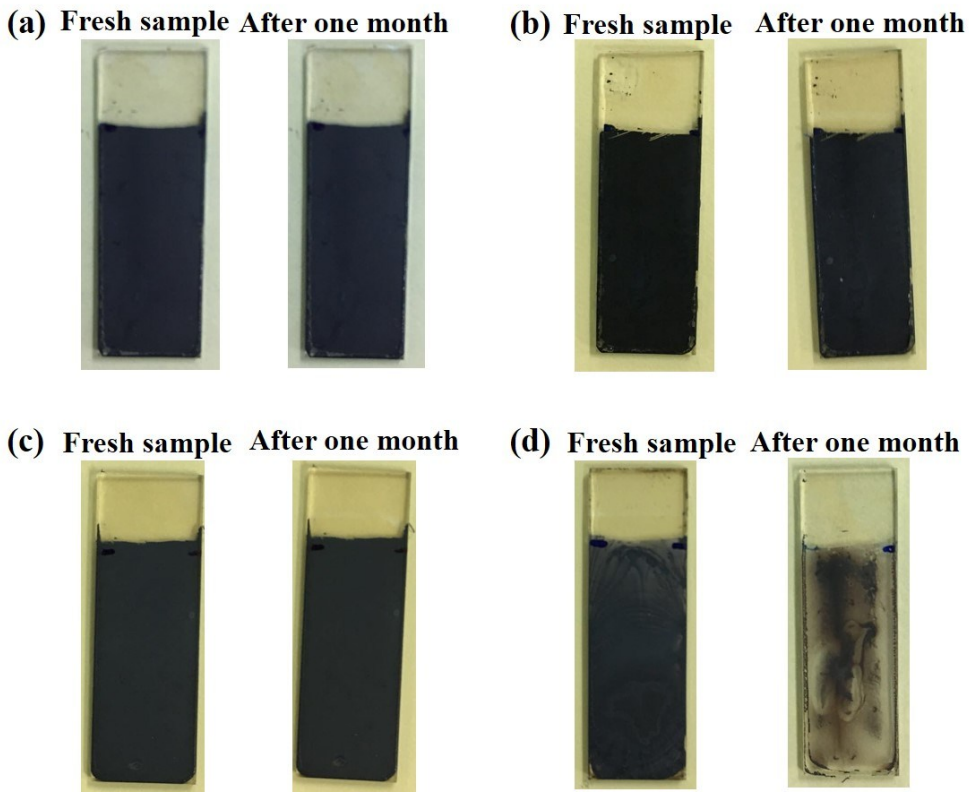

Fig. S15. Optical images of 2D $SnS_{2\text{-}4k}$ Ns-based photodeetctor measured in 0.1 M different electrolytes at 0 V or 0.6 V at IV level before and after one month. (a) 0.1 M Na_2SO_4, 0 V; (b) 0.1 M Na_2SO_4, 0.6 V; (c) 0.1 M H_2SO_4, 0.6 V; (d) 0.1 M KOH, 0.6 V.